Available online at www.sciencedirect.com
SCIENCE DIRECT
Polymer 47 (2006) 4936–4945
polymer
www.elsevier.com/locate/polymer

Soluble polyimides containing *trans*-diaminotetraphenylporphyrin: Synthesis and photoinduced electron transfer

Watchara Anannarukan [a], Supawan Tantayanon [b,*], Dong Zhang [c], Elvin A. Alemán [d], David A. Modarelli [d], Frank W. Harris [c]

[a] *Program of Petrochemistry, Faculty of Science, Chulalongkorn University, Bangkok 10330, Thailand*
[b] *Department of Chemistry, Faculty of Science, Chulalongkorn University, Bangkok 10330, Thailand*
[c] *The Maurice Morton Institute of Polymer Science, The University of Akron, Akron, OH 44325, USA*
[d] *Knight Chemical Laboratory, Department of Chemistry and The Center for Laser and Optic Spectroscopy, The University of Akron, Akron, OH 44325, USA*

Received 29 April 2006; received in revised form 9 May 2006; accepted 10 May 2006
Available online 2 June 2006

Abstract

5,15-Bis(4-aminophenyl)-10,20-diphenylporphyrin (*trans*-DATPP) was synthesized via the condensation of *meso*-(4-nitrophenyl)dipyrromethane and benzaldehyde. The further reaction with zinc acetylacetonate hydrate afforded zinc 5,15-bis(4-aminophenyl)-10,20-diphenylporphyrin (*trans*-ZnDATPP). A series of soluble polyimides based on *trans*-DATPP or *trans*-ZnDATPP, 2,2′-bis(trifluoromethyl)-4,4′-diaminobiphenyl (PFMB) and 4,4′-hexafluoroisopropylidenediphthalic anhydride (6FDA) at various ratios was then prepared. Some physical properties of these polyimides were measured. It was found that every polyimide containing either *trans*-DATPP or *trans*-ZnDATPP had higher viscosity than the polyimide without porphyrin unit. Furthermore, the polyimides with *trans*-ZnDATPP showed lower viscosity than the ones without *trans*-ZnDATPP at approximately the same porphyrin content. Glass transition temperatures (T_gs) of polyimides containing *trans*-ZnDATPP were higher than polyimides containing *trans*-DATPP, and both were higher than polyimide without porphyrin. Steady state fluorescence spectroscopy of these polymers revealed that the quantum yield of polymers increased with higher content of free base porphyrin in the polymer chain. Time-correlated single photon counting experiments indicated these polyimides could be used in photonic applications.

Keywords: Soluble polyimides; Diaminotetraphenylporphyrin; Photoinduced electron transfer

1. Introduction

Aromatic polyimides are known for their excellent mechanical and electrical properties [1] as well as their outstanding thermal stability [2,3]. They also display high softening temperatures and excellent chemical resistance. This combination of properties makes them ideal for use in commercial applications. However, aromatic polyimides are generally insoluble in common organic solvents. Thus, they must be processed in the form of their soluble poly(amic acid) (PAA) precursors, which are then chemically or thermally imidized in place. There are several drawbacks from the PAA approach. For example, water released during imidization can create weakening voids in thick parts of the material. Even with thin films, the thermal imidization process must be carefully controlled in order to minimize depolymerization and maximize the degree of imidization [4]. Therefore, a considerable amount of research aimed at the development of soluble aromatic polyimides has been carried out [2,3,5–7].

Porphyrin and its derivatives are well known as sensitizers in the photosynthesis of plants, and are frequently used in assemblies related to artificial solar energy conversion [8]. Various types of polymers containing porphyrins can therefore be used as photoresponsive materials [9], photorefractive materials [10], and molecular wires [11]. Recently, much attention has been paid to the synthesis of polyimides containing porphyrins, since they can be used potentially as photoconductive materials and charge transporting materials [12–15]. Although a few studies on photoinduced electron transfer in polyimides containing porphyrin had been reported [16–18], those polyimides were prepared via the imidization

* Corresponding author. Present address: Green Chemistry Research Lab, Department of Chemistry, Faculty of Science, Chulalongkorn University, Bangkok 10330, Thailand. Tel.: +66 2 218 5010; fax: +66 2 218 5038.
E-mail address: supawan.t@chula.ac.th (S. Tantayanon).

0032-3861/$ - see front matter © 2006 Elsevier Ltd. All rights reserved.
doi:10.1016/j.polymer.2006.05.023

of PAA films. In this work, we report the direct synthesis of polyimides containing free base porphyrin and zinc porphyrin that are soluble in common organic solvents. In addition, we report the optical properties (absorption, steady state and time resolved fluorescence) of these polymers; the data obtained from the fluorescence experiments enabled us to determine the approximate amount of photoinduced electron transfer in these soluble polymers. Because this information is more difficult to obtain for insoluble materials and films, the information obtained from these experiments is invaluable for the generation of new materials with improved properties and will be used for optimizing new porphyrin–diimide blends for new optical materials.

2. Experimental

2.1. Instrumentation

Proton nuclear magnetic resonance (^{1}H NMR) spectra were obtained with a Varian Gemini 300 MHz NMR spectrometer. ESI–QIT–MS was obtained with a Bruker Esquire-LC ion trap mass spectrometer. All melting points were determined on a Mel-Temp melting point apparatus and were uncorrected. IR spectra were recorded on a Nicolet NEXUS 870 FT-IR spectrometer equipped with a Thunderdom ATR accessory. Intrinsic viscosities were determined with SCHOTT-Ostwald viscometer (2 mL). Flow times were recorded for *N*-methyl-2-pyrrolidone (NMP) with polymer concentrations of approximately 0.2–1.0 g/dL at 35 °C ± 0.1. Absorption experiments were carried out on a Hitachi 3100 single monochromator UV–vis spectrophotometer. Steady state fluorescence measurements were run on a ISA Jobin Yvon-SPEX Fluorolog 3–22 fluorometer having dual input and output monochrometers. Fluorescence spectra were collected using argon-saturated solutions by exciting at the Soret band. Quantum yield measurements were made relative to tetraphenylporphyrin (TPP) and zinc tetraphenylporphyrin (ZnTPP). Thermogravimetric analyses (TGA) were obtained in nitrogen and air with a TA Hi-Res TGA 2950 thermogravimetric analyzer using heating rate of 10 °C/min. Glass transition temperature (T_gs) of polyimide films were determined with thermomechanical analysis (TMA) using a TA TMA 2940 thermomechanical analyzer with a tension mode, the films were subjected to three different stresses with heating rate of 10 °C/min. The T_g was taken as the temperature at which the slope of a plot of film dimensional change versus temperature occurred. The T_gs obtained at each stress level were then extrapolated to zero stress.

2.2. Time-resolved fluorescence experiments

All solvents used for spectroscopic measurements were either Spectral or HPLC grade. Time-resolved fluorescence experiments were performed using the time-correlated single photon counting (TCSPC) technique. The instrument used in this work utilized the pulses from a Coherent cavity dumped 702 dye laser pumped by the 527 nm output of a Quantronix 4417 CW mode-locked Nd:YLF laser. The fluorescence signal was detected at 54.7° with an emission polarizer and depolarizer, using a Hamamatsu R3809U-51 red-sensitive multichannel plate detector (MCP). Data collection and analysis was accomplished with an Edinburgh Instruments data collection system, with resolution estimated at ~7–9 ps. Fluorescence decays having multiple components were fit using the Marquardt algorithm. Most measurements were fit such that values of $\chi^2 < 1.20$ were obtained, although some fits were made to $\chi^2 < 1.40$ due the complexity of the decays and the limitations of our data analysis software. Error limits in these measurements are typically ±10%. All TCSPC experiments were run with argon-saturated CH_2Cl_2 and DMAc solutions with an optical density of 0.15 at the excitation wavelength of 573 nm. The decay profile of PI-3 was monitored at 650 nm and the decay profile of PI-6 was monitored at 610 nm.

Electron-transfer rate constants were calculated using Eq. (1)

$$k_{ET} = 1/\tau_{PI} - 1/\tau_{ref} \quad (1)$$

where τ_{PI} represents the fluorescence lifetime of polyimides and includes contributions from each fluorescence lifetime, such that $\tau_{PI} = a_1(\tau_1) + a_2(\tau_2)$, and a_1 and a_2 represent the pre-exponential factors for each component as determined by the equation: $a_i = (a_i\tau_i / \sum a_i\tau_i)100$.

2.3. Electrochemistry

Cyclic voltammograms (CV) were recorded on a BAS-100 electrochemistry apparatus from Bioanalytical System, Inc. at 20 °C. A three-electrode configuration was used with platinum working and auxiliary electrodes, and the standard calomel electrode as a reference (0.1 M supporting electrolyte, tetrabutylammonium perchlorate, TBAP).

2.4. Materials

Pyrrole (Acros) was distilled over calcium hydride under reduced pressure. Benzaldehyde (EMD) and isoquinoline (Aldrich) were distilled under reduced pressure. Dichloromethane (CH_2Cl_2) (EMD) was distilled over calcium hydride. *N*-Methyl-2-pyrrolidone (NMP) (Aldrich) was distilled from phosphorous pentoxide under reduced pressure. 4,4′-Hexafluoroisopropylidenediphthalic anhydride (6FDA) is purchased from Daikin and sublimed before used. All of other reagents and solvents were used as received.

3. Monomer syntheses

3.1. Meso-(4-nitrophenyl)dipyrromethane (*1*)

Dipyrromethane was synthesized with the standard procedure in the literature [19]. A mixture of 4-nitrobenzaldehyde (0.511 g, 1 mmol) and pyrrole (2.8 mL, 40 mmol) was degassed with N_2 for 15 min, then trifluoroacetic acid (8 μL, 0.1 mmol) was added. The solution was stirred for 30 min at

room temperature, at which point no starting aldehyde was shown by TLC analysis. The mixture was diluted with dichloromethane (50 mL) then washed with 0.1 M sodium hydroxide (2×25 mL), washed with water and dried with anhydrous sodium sulfate. The solvent was removed under reduced pressure and then the unreacted pyrrole was removed by vacuum distillation at room temperature. The crude product was precipitated from CH_2Cl_2/hexane and then recrystallized from ethanol/water to afford the yellow solid **1b**. (0.2 g, 75%): mp 163–165 °C (Ref. 159–160 °C [20]), IR (KBr): 3390 (NH), 3353 (NH), 1512 (C–NO_2), 1348 (NO_2), 857 (1,4-subst. benzene) cm^{-1}; ^1H NMR ($CDCl_3$) δ: 8.17 (d, 2H), 8.01 (br s, 2H), 7.37 (d, 2H), 6.74–6.71 (m, 2H), 6.17 (q, 2H), 5.86–5.83 (m, 2H), 5.57 (s, *meso*-H) ppm.

3.2. 5,15-Bis(4-nitrophenyl)-10,20-diphenylporphyrin (*2*)

5,15-Bis(4-nitrophenyl)-10,20-diphenylporphyrin was synthesized by the reaction of **1** and benzaldehyde as starting reactant, in accordance with the method of Lindsey et al. [19]. A solution of *meso*-(4-nitrophenyl)dipyrromethane (1.068 g, 4 mmol) and benzaldehyde (0.4245 g, 4 mmol) in 400 mL CH_2Cl_2 was purged with N_2 for 15 min, then $BF_3 \cdot OEt_2$ (0.6 mL of 2.5 M stock solution in CH_2Cl_2) was added. The solution was stirred for 90 min at room temperature, then 2,3-dichloro-5,6-dicyanobenzoquinone (DDQ) (0.6810 g, 3 mmol) was added. The mixture was stirred at room temperature for an additional 90 min and the solvent was removed until the amount of solvent is maintained about 50 mL. It was then pre-adsorbed on silica gel and flash chromatography (silica, CH_2Cl_2:hexane = 60:40) gave compound **2** (0.1341 g, 4.76%): mp > 300 °C, IR (KBr): 3315 (NH), 1517 (asym, C–NO_2), 1343 (sym, C–NO_2), 962 (NO_2), 847 (1,4 subst. benzene) cm^{-1}; ^1H NMR ($CDCl_3$) δ: 8.90 (d, 4H, β-H), 8.75 (d, 4H, β-H), 8.65 (d, 4H, nitrophenyl), 8.40 (d, 4H, nitrophenyl), 8.21 (d, 4H, *o*-phenyl), 7.78–7.75 (m, 6H, *p*-, *m*-phenyl), −2.81 (s, 2H, internal NH) ppm.

3.3. 5,15-Bis(4-aminophenyl)-10,20-diphenylporphyrin (*3*)

The reduction of **2** was conducted according to the modification of Kruper's procedure [21]. Compound **2** (0.4370 g, 0.6201 mmol) was dissolved in 220 mL of concentrated hydrochloric acid under nitrogen. Tin (II) chloride dihydrate (1.1193 g, 4.9608 mmol) was added to the solution, and the reaction was heated to 65 °C for 90 min. The porphyrin solution was cooled to room temperature and poured into ice water and was adjusted to pH 8 with concentrated ammonium hydroxide. The aqueous phase was extracted with 5×200 mL portions of CH_2Cl_2, which were combined and dried over anhydrous magnesium sulfate. The organic phase was concentrated on a rotary evaporator to 50 mL and this solution was pre-adsorbed on silica gel. Flash chromatography (silica, 10% EtOAc in CH_2Cl_2) gave compound **3** (*trans*-DATPP) as the purple crystal. (0.3294 g, 28%): mp > 300 °C, IR (KBr): 3370 (NH_2), 3326 (NH), 1515 (NH_2-bend), 800 (1,4-subst. benzene) cm^{-1}; ^1H NMR (DMSO-d_6) δ: 8.95 (d, 4H, β-H), 8.76 (d, 4H, β-H), 8.22 (d, 4H, aminophenyl), 7.87–7.80 (m, 10H, phenyl), 7.03 (d, 4H, aminophenyl), 5.59 (s, 4H,NH_2), −2.81 (s, 2H, internal NH) ppm; UV–vis (CH_2Cl_2) λ_{max} (log ε): 423 (5.27), 520 (3.88), 558 (3.75), 595 (3.42), 652 (3.48) nm; ESI–QIT–MS: 645.1 $[M+H]^+$ (calculated for $C_{44}H_{32}N_6$: 644.77).

3.4. Zinc 5,15-bis(4-aminophenyl)-10,20-diphenylporphyrin (*4*)

To a solution of 190 mL of THF was added **3** (638 mg, 0.9895 mmol) and zinc acetylacetonate hydrate (1.276 g, 4.5331 mmol) [17]. The solution was refluxed for 4 h, cooled to room temperature, and then the solvent was evaporated. The precipitate was partly dissolved in methanol solution by heating and left overnight at 0 °C. The resulting violet crystal was collected, washed with methanol, and then dried to afford *trans*-ZnDATPP, **4**, (0.56 g, 80%): mp > 300 °C; ^1H NMR (DMSO-d_6) δ: 8.91 (d, 4H, β-H), 8.75 (d, 4H, β-H), 8.19 (d, 4H, aminophenyl), 7.84–7.78 (m, 10H, phenyl), 6.99 (d, 4H, aminophenyl), 5.45 (s, 4H, NH_2) ppm; UV–vis (CH_2Cl_2) λ_{max} (log ε): 423 (5.47), 550 (4.18), 589 (3.79) nm; ESI–QIT–MS: 709.2 $[M+H]^+$ (calculated for $C_{44}H_{30}N_6Zn$: 708.14).

3.5. 2,2′-Bis(trifluoromethyl)-4,4′-diaminobiphenyl (***PFMB***)

The compound was prepared from 2-bromo-5-nitrobenzotrifluoride or 2-iodobenzotrifluoride by the described procedure [22,23]: mp 180–182 °C (Refs. 181–182 °C [22,23]).

3.6. General procedure for polymer syntheses

The dianhydride monomer (6FDA) (0.93 mmol) was added to the diamino monomer (0.93 mmol), PFMB/*trans*-DATPP (**3**)/*trans*-ZnDATPP (**4**), at various mole ratios in dry NMP containing a small amount of isoquinoline under nitrogen at ambient temperature. After the solution was stirred for 8 h, it was heated to reflux and maintained at that temperature for 12 h. After the solution was allowed to cool to ambient temperature, it was slowly added to vigorously stirred methanol. The precipitated polymer was collected by filtration, washed with methanol, and dried under reduced pressure at 200 °C for 24 h. The polymer was obtained in 90–95% yield.

4. Results and discussion

4.1. Monomer syntheses

In general, 5,15-bis(4-aminophenyl)-10,20-diphenylporphyrin (*trans*-DATPP) can normally be synthesized by two steps, the formation and subsequent reduction of 5,15-bis(4-nitrophenyl)-10,20-diphenylporphyrin (dinitro-compound). The synthesis of the dinitro-compound can be carried out by three routes; the direct reaction of pyrrole, benzaldehyde and 4-nitrobenzaldehyde [12], the nitration of tetraphenylporphyrin [24] and the two-step reaction of pyrrole and aldehyde via the formation of *meso*-substituted

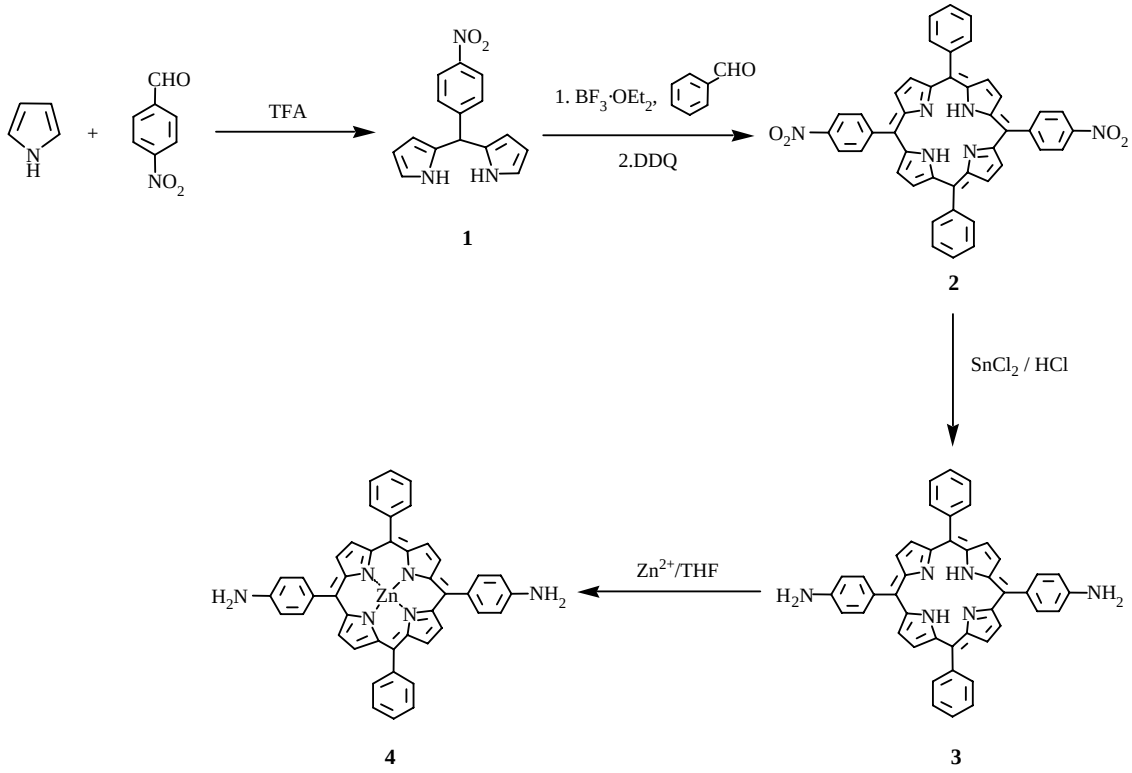

Scheme 1. Monomer syntheses.

dipyrromethane [19]. In this research, the *trans*-DATPP was synthesized via *meso*-substituted dipyrromethane.

The synthesis of *trans*-DATPP was attempted by starting from the condensation between pyrrole and either benzaldehyde or 4-nitrobenzaldehyde with the catalytic amount of trifluoroacetic acid at room temperature. The complete reaction was obtained when no aldehyde left in the reaction as monitored by TLC. The excess pyrrole was recovered by vacuum distillation at room temperature. When benzaldehyde was used, column chromatography on silica was required to isolate the white *meso*-phenyldipyrromethane with 30% yield. The reaction with 4-nitrobenzaldehyde, however, afforded *meso*-(4-nitrophenyl)dipyrromethane (**1**), which was precipitated after adding the reaction mixture into CH_2Cl_2/hexane and recrystallized in aqueous ethanol with 75% yield. Therefore, *meso*-(4-nitrophenyl)dipyrromethane has been selected for further reaction with benzaldehyde to obtain 5,15-bis(4-nitrophenyl)-10,20-diphenylporphyrin (**2**) with 4% yield (Scheme 1). This low percentage yield was attributed to the effect of the nitro-group on **1** to its condensation reaction with benzaldehyde [24]. Lastly, **2** was reduced by using tin (II) chloride dihydrate and concentrated hydrochloric acid [21] and subsequently subjected to column chromatography to obtain pure 5,15-bis(4-aminophenyl)-10,20-diphenylporphyrin (*trans*-DATPP, **3**) with 28% yield (Scheme 1). Its structure was identified by FT-IR and ^{1}H NMR spectroscopy.

The incorporation of zinc into free base porphyrin, *trans*-DATPP, was performed by reacting with zinc acetylacetonate hydrate. The formation of zinc 5,15-bis(4-aminophenyl)-10,20-diphenylporphyrin (*trans*-ZnDATPP, **4**) was confirmed by its infrared spectrum, where the disappearance of the absorption band at 3318 cm^{-1} due to the internal ν(NH) stretching for *trans*-DATPP was observed. In addition, the ^{1}H NMR spectrum of *trans*-DATPP (Fig. 1(a)) showed the characteristic internal NH at −2.81 ppm, while the disappearance of this signal in the ^{1}H NMR spectrum of *trans*-ZnDATPP was observed, which clearly indicated that zinc had bound with *trans*-DATPP (Fig. 1(b)).

4.2. Polymer syntheses

Trans-DATPP or *trans*-ZnDATPP was polymerized with PFMB and 6 FDA (Scheme 2) at various mole ratios (Table 1) in NMP containing catalytic amount of isoquinoline. The polymerization was initially carried out at ambient temperature for 8 h. The resulting poly(amic acid) was not isolated and the polymerization solution was further heated at reflux for 12 h. During this time, the water generated from imidization was allowed to distill from the reaction mixture to favor the polyimide formation. The polyimide product, which remained in solution throughout the polymerization, was isolated by precipitation in methanol. Typical IR spectra of these polyimides are shown in Fig. 2. The characteristics of amine absorption band (from the amine monomer) and amide absorption band (from PAA) were not observed, whereas the characteristic absorption bands for the polyimide were observed at 1787, 1732, 1367 and 721 cm^{-1}. The internal NH of polyimides containing *trans*-DATPP could not be observed due to the small amount of *trans*-DATPP incorporated into the polymer.

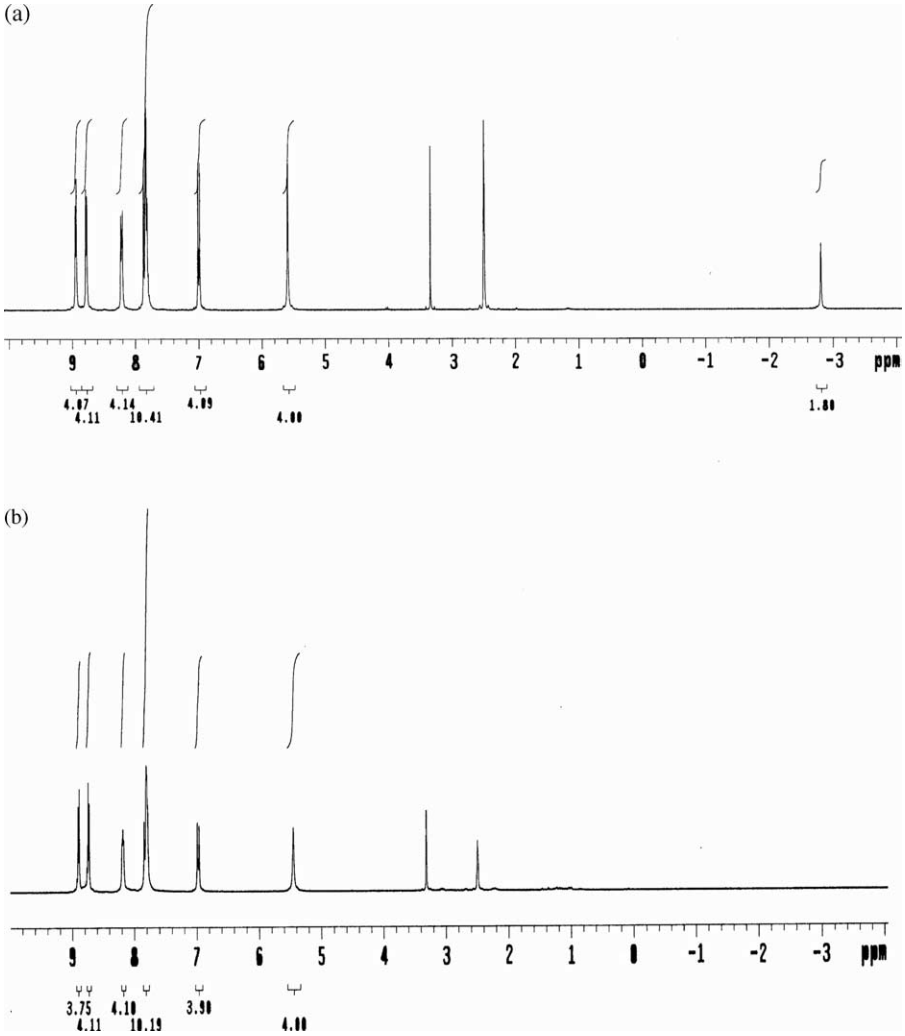

Fig. 1. ^{1}H NMR (DMSO-d_6) (a) *trans*-DATPP and (b) *trans*-ZnDATPP.

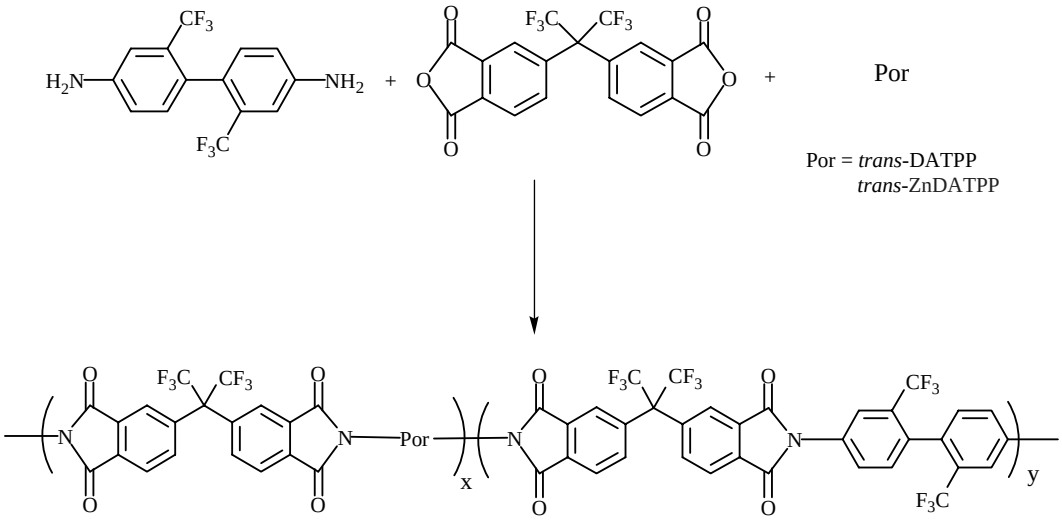

Scheme 2. Polymer syntheses.

Table 1
Resulting data of the syntheses of polyimides

PI	mol%			$[\eta]^a$ (dL/g)	$T_g{}^b$ (°C)	TGA[c] (°C)	
	6FDA	PFMB	DATPP/ ZnDATPP			N_2	Air
PI-0	100	100	–	0.72	284	492	462
trans-DATPP							
PI-1	100	95	5	1.10	294	492	487
PI-2	100	90	10	0.95	301	502	475
PI-3	100	85	15	0.90	310	501	467
trans-ZnDATPP							
PI-4	100	95	5	0.99	316	488	455
PI-5	100	90	10	0.81	318	477	456
PI-6	100	85	15	0.76	326	486	449

[a] Intrinsic viscosity determined in NMP at 35 °C.
[b] Temperature at which change in slope occurred on a plot of film dimensional change versus temperature obtained by TMA with a heating rate of 10 °C/min. Films were subjected to three different initial stresses and the results were extrapolated to zero stress.
[c] Temperature at which 5% weight loss occurred when polymers were subjected to TGA with a heating rate of 10 °C/min.

4.3. Polymer properties

4.3.1. Solution properties

Table 1 shows the intrinsic viscosities of the polyimides measured in NMP at 35 °C. All the polyimides containing *trans*-DATPP or *trans*-ZnDATPP had a higher viscosity than the polyimide without porphyrin. It is possible that much higher molecular weights of polymers were obtained when porphyrins were incorporated into the polyimide chains. However, it has been reported that strong attractive interactions between porphyrins can lead to aggregation in solution [25]. Intrachain aggregation within the polyimide via π–π interactions of porphyrins on the same chain is expected to result in a decrease in viscosity with increasing porphyrin content (greater coiling), whereas interchain aggregation is expected to result in an increase in viscosity through increased chain entanglement. Therefore, both inter- and intra-interactions of the polyimide chains would attribute to the higher viscosity compared to the polyimide without porphyrin. A decrease in viscosity with increasing porphyrin concentrations in both *trans*-DATPP and *trans*-ZnDATPP-containing polyimides was observed, indicating probable intrachain interactions (i.e. coiling). Interestingly, polyimides containing *trans*-ZnDATPP had lower viscosities than those containing *trans*-DATPP at the same level of porphyrin content, a result that can be attributed to ligation of the zinc porphyrin with either the polymer or the solvent [25,26,30,31]. Currently, the aggregation of these polyimides is under investigation.

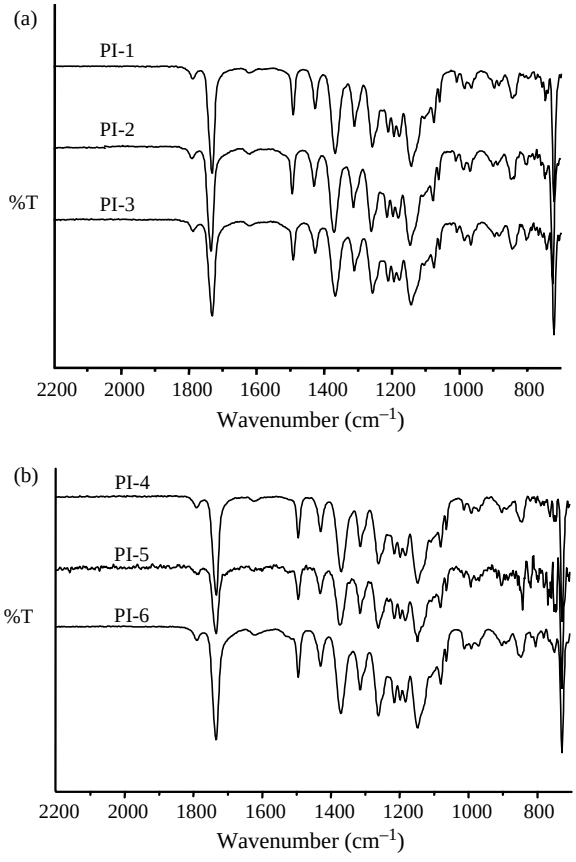

Fig. 2. FT-IR spectra of polyimides containing (a) free base porphyrin and (b) zinc porphyrin.

4.3.2. Thermal properties

These polyimides displayed good thermal and thermooxidative stabilities. They had 5% weight losses at 477–502 °C in nitrogen and at 449–487 °C in air (Table 1). The polyimides containing *trans*-DATPP seem slightly more stable than polyimides containing *trans*-ZnDATPP at the same level of porphyrin content. From the TGA data, it was found that the existence of *trans*-DATPP or *trans*-ZnDATPP in the polymer did not significantly affect the thermal stabilities of these polyimides. The T_gs of the polyimides were obtained from TMA measurements on polyimide films, which were casted from their THF solutions (Table 1). It was found that T_gs of all polyimides containing *trans*-ZnDATPP are higher than the polyimides containing *trans*-DATPP at the same amount of porphyrin. This is due to the incorporation of *trans*-ZnDATPP in polymer structure made the polymer structure more rigid than polymer containing *trans*-DATPP. Polyimide without porphyrin showed the lower T_g than polyimides containing *trans*-DATPP or *trans*-ZnDATPP. This could be attributed to the higher polymer chain flexibility.

4.3.3. Solubility

The solubility behavior of the polyimides is summarized in Table 2. All polyimides based on 6FDA and PFMB were

Table 2
Solubility of polyimides

Polymer	NMP	DMAc	DMSO	DMF	THF	Acetone	CH_2Cl_2
PI-1	++	++	++	++	++	++	+
PI-2	++	++	++	++	++	++	+
PI-3	++	++	++	++	++	++	+
PI-4	++	++	++	++	++	++	+
PI-5	++	++	++	++	++	++	+
PI-6	++	++	++	++	++	++	+

Polyimide solutions at 4% w/v at room temperature. ++, highly soluble; +, moderately soluble.

Table 3
Electrochemical data for TPP, ZnTPP, PI-3 and PI-6

Compound	$E_{1/2}$ (ox)[a]	$E_{1/2}$ (red)[b]	E_s[c]	ΔG_{ET}[d]
TPP	1.03[e]		1.91	
PI-3		−1.25	1.91	0.37
ZnTPP	0.78[e]		2.10	
PI-6		−1.14		−0.17

In CH_2Cl_2, TBAP as an electrolyte.
[a] Volts, See Ref. [30].
[b] Volts, reference VS SCE reference elctrode.
[c] Estimated in the usual manner from the wavelengths of the longest Q-band absorption and $S_1 \rightarrow S_0$ emission.
[d] Estimated using the Weller equation ($\Delta G_{ET} = E_{ox} - E_{red} - E_s$), from the values recorded using SCE reference electrode.
[e] See Ref. [30].

soluble in many polar aprotic solvents (DMAc, DMF, NMP, DMSO), an ether solvent (THF), and ketone solvent (acetone). Because the polyimide chain packing was interfered by the steric hindrance of hexafluoroisopropylidene group and the twist of PFMB unit due to the trifluoromethyl groups at 2 and 2′ positions resulting in high free volume and low crystallinity of polyimides and made them soluble. The similar phenomenon has already been reported by other research groups [2,3,27–29]. However, this is the first report of the soluble polyimides containing porphyrin.

4.3.4. Electrochemistry

Cyclic voltammetry (CV) measurements were performed on the polyimides containing the highest mole percent of porphyrin (i.e. PI-3 and PI-6). The reduction potentials, $E_{1/2}$ (red), for these polymers are shown in Table 3. Unfortunately, the oxidation potentials $E_{1/2}$ (ox) for these polymers could not be determined, possibly because the porphyrin moieties were not accessible to the electrode surface [30]. The free energy of electron transfer (ΔG_{ET}) was therefore calculated using the first singlet excited state energy of the porphyrin donor, the value of $E_{1/2}$ (red) determined in this work and literature values of $E_{1/2}$ (ox) [30]. For PI-3, ΔG_{ET} is estimated to be endothermic by ~0.37 eV, whereas the corresponding value for the zinc porphyrin-containing polymer (PI-6) was calculated to be exothermic by −0.17 eV.

4.3.5. Spectroscopic properties

The good solubility of these polymers enabled us to investigate the photophysical processes of these polymers (i.e. absorption, excitation and photoinduced electron transfer processes). Absorption spectra (Fig. 3, Table 4) obtained for polyimides containing *trans*-DATPP (PI-1–PI-3) and *trans*-ZnDATPP (PI-4–PI-6) are more similar to each other and to tetraphenylporphyrin (TPP) and zinc tetraphenylporphyrin (ZnTPP) than the starting monomers (*trans*-DATPP and *trans*-ZnDATPP, respectively). The Soret bands for polymers containing *trans*-DATPP are observed at 419 nm in CH_2Cl_2 and 418 nm in DMAc, while TPP absorbs at 417 nm in both CH_2Cl_2 and DMAc. In the case of polymers containing *trans*-ZnDATPP, the Soret bands are observed at 420 nm in CH_2Cl_2 and 427 nm in DMAc, while ZnTPP is observed at 418 nm in CH_2Cl_2 and 426 nm in DMAc.

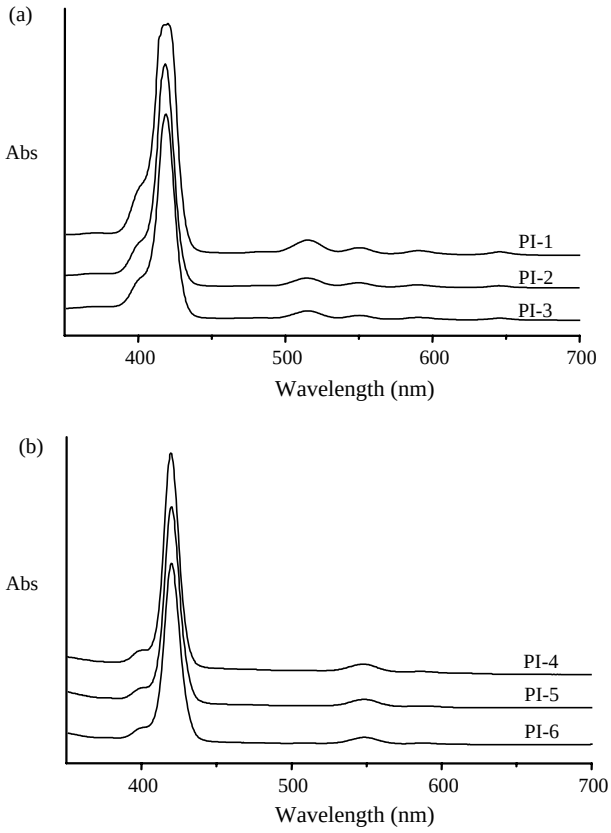

Fig. 3. UV–vis absorption spectra (CH_2Cl_2) of polyimides containing (a) free base porphyrin and (b) zinc porphyrin.

Steady state fluorescence measurements were performed on both polyimides containing *trans*-DATPP and *trans*-ZnDATPP. Similar to the absorption spectra, very little change is observed in the energies of the fluorescence bands for polyimides containing *trans*-DATPP (PI-1–PI-3), which have

Table 4
UV–vis absorption maxima of polyimides in CH_2Cl_2 and DMAc

Compound	CH_2Cl_2		DMAc	
	Soret band (nm)	Q-band (nm)	Soret band (nm)	Q-band (nm)
TPP	417	515, 549, 590, 646	417	514, 548, 590, 646
trans-DATPP	423	520, 558, 595, 652	425	522, 567, 600, 660
PI-1	419	515, 550, 590, 646	418	515, 550, 590, 646
PI-2	419	515, 550, 590, 646	418	515, 550, 590, 646
PI-3	419	515, 550, 590, 646	418	515, 550, 590, 646
ZnTPP	418	548, 585	426	560, 599
trans-ZnDATPP	423	550, 589	432	562, 607
PI-4	420	548, 588	427	560, 600
PI-5	420	548, 588	427	560, 600
PI-6	420	548, 588	427	560, 600

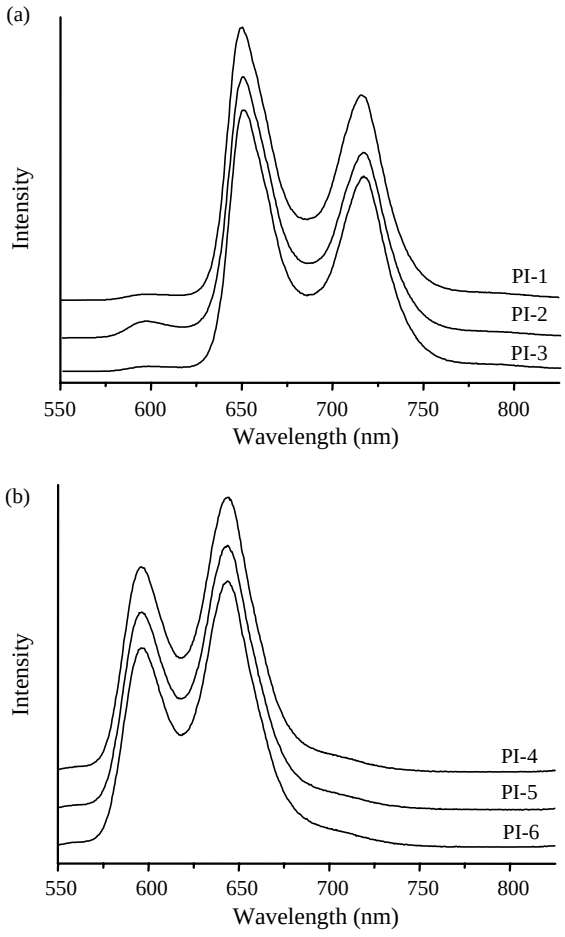

Fig. 4. Fluorescence spectra (CH_2Cl_2) of polyimides containing (a) free base porphyrin and (b) zinc porphyrin.

fluorescence bands at 650 and 714 nm in CH_2Cl_2, and 650 and 715 nm in DMAc (Fig. 4(a), Table 5). These bands are nearly identical to those observed for TPP in the same solvents (649 and 714 nm in CH_2Cl_2, 650 and 715 nm in DMAc). The quantum yields for these polymers were also determined, and are shown in Table 6. Because substitution on the porphyrin changes the quantum yield of the porphyrin standard substantially, relative quantum yields ($\Phi_{PI-n}/\Phi_{trans\text{-DATPP}}$ and $\Phi_{PI-n}/\Phi_{trans\text{-ZnDATPP}}$, where $n=1$–3 for the free base porphyrin-containing polyimides and $n=4$–6 for the zinc porphyrin-containing polyimides) are also shown in Table 6. As expected, the fluorescence quantum yield for the free base

Table 5
Fluorescence maxima of polyimides in CH_2Cl_2 and DMAc

Compound	CH_2Cl_2	DMAc
TPP	649, 714	650, 715
PI-1	650, 714	650, 715
PI-2	650, 714	650, 715
PI-3	650, 714	650, 715
ZnTPP	593, 643	604, 660
PI-4	596, 643	606, 660
PI-5	596, 643	606, 660
PI-6	596, 643	606, 660

Table 6
Quantum yield of polyimides

Compound	CH_2Cl_2		DMAc	
	Φ_{Fl}	$\Phi_{PI-n}/\Phi_{trans\text{-DATPP}}$ or $\Phi_{PI-n}/\Phi_{trans\text{-ZnDATPP}}$	Φ_{Fl}	$\Phi_{Fl}/\Phi_{trans\text{-DATPP}}$ or $\Phi_{Fl}/\Phi_{trans\text{-ZnDATPP}}$
TPP	0.11		0.15	
Trans-DATPP	0.16		0.19	
PI-1	0.071	0.44	0.16	0.84
PI-2	0.084	0.53	0.18	0.95
PI-3	0.089	0.56	0.19	1.0
ZnTPP	0.03		0.03	
trans-ZnDATPP	0.054		0.033	
PI-4	0.021	0.39	0.022	0.67
PI-5	0.020	0.37	0.020	0.61
PI-6	0.017	0.31	0.017	0.51

porphyrin-containing polymers, PI-1–PI-3, increased slightly with an increasing percentage of free base porphyrin in both CH_2Cl_2 and DMAc. In CH_2Cl_2, the quantum yields are decreased substantially relative to TPP (19–35%), indicating significant quenching of the porphyrin fluorescence that is attributed to electron transfer from a porphyrin donor to a diimide acceptor group. The relative quantum yield data indicate quenching via electron transfer is ~44–56% efficient. In contrast, the quantum yields Φ_{PI-n} in DMAc are slightly larger than that of TPP; the relative quantum yield data indicates only a small (0–15%) amount of fluorescence quenching compared to the starting porphyrin.

The fluorescence spectra of the polyimides containing *trans*-ZnDATPP (PI-4–PI-6) also parallel their absorption spectra (Fig. 4(b), Table 5). Thus, a red-shift in the fluorescence maxima from that of ZnTPP (593 and 643 nm in CH_2Cl_2, 604 and 660 nm in DMAc) is observed in the fluorescence spectra of polyimides PI-4–PI-6. Fluorescence maxima at 596 and 643 nm are found for polyimides in CH_2Cl_2, and maxima at 606 and 660 nm were observed in DMAc. These spectral shifts are unlike those observed for polyimides containing *trans*-DATPP, which showed only very little change in fluorescence maxima. Interestingly, the quantum yields of fluorescence were not affected by the increase of *trans*-ZnDATPP content in the polymer backbone (Table 6). The small red shift (2–3 nm) observed for polymers containing zinc porphyrin in CH_2Cl_2 and DMAc can be attributed to a combination of pi-stacking and a dynamic complexation of zinc porphyrin with either the solvent or other regions of the polymer chain [30]. Fluorescence quantum yields of zinc porphyrin-containing polyimides, PI-4–PI-6, show substantial fluorescence quenching in both solvents. In CH_2Cl_2, the amount of quenching is ~30–43% of ZnTPP and ~60–70% of that of the monomeric porphyrin, and in DMAc the quenching is ~27–43% of ZnTPP and ~33–49% of the monomer.

Fluorescence lifetimes (τ_{Fl}) for the two polymers containing *trans*-DATPP, PI-3 and *trans*-ZnDATPP, PI-6 were determined using the time-correlated single photon counting (TCSPC) technique, and are shown in Table 7. The fluorescence lifetimes were found to be best to a two-component exponential decay composed of one major component and one minor component. The values of τ_{Fl} for both polymers

Table 7
Summary of photophysical data of polyimides

Compound	Solvent	τ_1[a] (ns)	τ_2[a] (ns)	k_{ET} (s^{-1})
TPP	CH_2Cl_2	9.25[b]		
ZnTPP	CH_2Cl_2	1.78[b]		
PI-3	CH_2Cl_2	8.22 (99.02%)	0.94 (0.98%)	1.35×10^7
PI-6	CH_2Cl_2	1.51 (96.75%)	0.37 (3.25%)	1.17×10^8
TPP	DMAc	12.2[b]		
ZnTPP	DMAc	1.92[b]		
PI-3	DMAc	10.70 (98.38%)	1.74 (1.62%)	1.28×10^7
PI-6	DMAc	1.53 (96.99%)	0.48 (3.01%)	1.46×10^8

[a] Values in parentheses are the relative contribution from each component.
[b] See Ref. [30].

were uniformly smaller than those of the model compounds. The major component for PI-3 was found to be 8.22 ns in CH_2Cl_2 and 10.70 ns in DMAc, both values of which are smaller than those of TPP (9.25 ns in CH_2Cl_2 and 12.2 ns in DMAc), while the major component in polymer PI-6 was 1.51 ns in CH_2Cl_2 and 1.53 ns in DMAc (compared to 1.78 ns for ZnTPP in CH_2Cl_2 and 1.92 ns in DMAc). From these lifetimes the electron transfer rate constants (k_{ET}, Table 7) were determined for each polymer Eq. (1), assuming electron transfer is the sole method of excited state decay other than fluorescence. From this data, it is seen that the rate constants determined for PI-3 are similar to one another in both solvents, but are approximately an order of magnitude smaller than those of PI-6. The fluorescence quantum yield and lifetime data can now be assessed in terms of the corresponding electrochemical data. The endothermic value of ΔG_{ET} obtained for the free base porphyrin-containing polymers indicates ET is unlikely in these polymers. Nonetheless, a small to moderate decrease in both Φ_{Fl} and τ_{Fl} is observed for PI-1–PI-3. A possible explanation for these values is that chain coiling in CH_2Cl_2 leads to a favorable spatial arrangement of the donor porphyrin and the acceptor diimide group for ET. More extensive chain coiling is expected in a poor solvent, wherein the polymer is better solvated by itself than by the solvent. The poorer solubility of the polymer in CH_2Cl_2, that leads to lower values of Φ_{Fl} and more rapid k_{ET}, supports this explanation. Alternatively, the aforementioned aggregation effects might serve to change the local environment around the porphyrin macrocycle in the polymer, making ET more favorable than calculated in Table 3. In the case of the zinc porphyrin-containing polymer, PI-6, electron transfer is clearly a favorable pathway for excited state decay. The lower value of Φ_{Fl} and more rapid k_{ET} in CH_2Cl_2 relative to DMAc for the zinc porphyrin-containing polymers appears to support the first interpretation, where coiling effects have a much larger impact on electron transfer than local changes in the redox properties of the donor and acceptor groups.

5. Conclusions

A series of polyimides containing either *trans*-DATPP or *trans*-ZnDATPP were synthesized and found to be soluble in most common organic solvents. These porphyrin-containing polyimides exhibited significantly higher viscosities than polyimide without porphyrin. We postulate that the aggregation of polyimide chains occurs via π–π interaction of porphyrin units, and in the case of the zinc porphyrin-containing polyimides, axial ligation to the zinc porphyrin. The excellent solubility of these polyimides provides several advantages compared to insoluble porphyrin-containing polyimides, including the capability to study their photophysical properties in solution. Steady state and time-resolved fluorescence measurements on these polymers in CH_2Cl_2 and DMAc revealed moderate quenching of the fluorescence that was attributed to photoinduced electron transfer from excited porphyrin units within the polymer to diimide acceptor groups. In future work, we intend to optimize both the electron transfer properties of these polymers by modifying both the acceptor group as well as the ratio of porphyrin/acceptor within the copolymer. Polymers of this type have great potential in photonic applications, and it is clear that being able to evaluate their photoinduced processes in solution will be beneficial to understanding their solid state-thin film properties.

Acknowledgements

The support of this work was supported by Thailand Research Fund (TRF), The Royal Golden Jubilee Scholarship, Grant no. PHD/0029/2544. The authors are grateful to The Maurice Morton Institute of Polymer Science, The University of Akron for some research facilities. D.A.M. gratefully acknowledges the National Science Foundation (CHE-0216371 and CHE-9816260) for support.

References

[1] Arnold Jr FE, Cheng SZD, Hsu SL-C, Lee CJ, Harris FW. Polymer 1992; 33:5179.
[2] Harris FW, Lin S-H, Li F, Cheng SZD. Polymer 1996;37:5049.
[3] Lin S-H, Li F, Cheng SZD, Harris FW. Macromolecules 1998;31:2080.
[4] Harris FW. In: Wilson D, Stenzenberger HD, Hergenrother PM, editors. Polyimides. New York: Chapman and Hall; 1990. p. 1.
[5] Kim YJ, Chung IS, Sang II, Kim SY. Polymer 2005;46:3992.
[6] Yin D, Li Y, Shao Y, Zhao X, Yang S, Fan L. J Fluorine Chem 2005; 126:819.
[7] Yang C-P, Su Y-Y, Hsiao F-Z. Polymer 2004;45:7529.
[8] Chou J-H, Kosal ME, Nalwa HS, Rakow NA, Suslick KS. In: Kadish K, Smith K, Guilard R, editors. The porphyrin handbook, vol. 6. New York: Academic Press; 2000. p. 43.
[9] Bao Z, Chen Y, Yu L. Macromolecules 1994;27:4629.
[10] Peng Z-H, Bao Z, Yu L. J Am Chem Soc 1994;116:6003.
[11] Wagner RW, Lindsey JS. J Am Chem Soc 1994;116:9759.
[12] Nisiukata Y, Morikawa A, Kakimoto M-A, Imai Y, Nishiyama K, Fujihira M. Polym J 1990;22:593.
[13] Xu Z-K, Zhu B-K, Xu Y-Y. Chem Mater 1998;10:1350.
[14] Zhu B-K, Xu Z-K, Xu Y-Y. Eur Polym J 1999;35:77.
[15] Zhu B-K, Xu Y-Y, Wei X-Z, Xu Z-K. Polym Int 2004;53:708.
[16] Iwamoto M, Xu X. Thin Solid Films 1996;284–285:936.
[17] Ohkita H, Ogi T, Kinoshita R, Ito S, Yamamoto M. Polymer 2002;43: 3571.
[18] Ogi T, Kinoshita R, Ito S. J Colloid Interface Sci 2005;286:280.
[19] Lee C-H, Lindsey JS. Tetrahedron 1994;50:11427.
[20] Littler BJ, Miller MA, Hung C-H, Wagner RW, ÓShea DF, Boyle PD, et al. J Org Chem 1999;64:1391.

[21] Kruper Jr WJ, Chamberlin TA, Kochanny M. J Org Chem 1989;54: 2753.
[22] Roger HG, Gaudiana RA, Hollinsed WC, Kalyanaraman PS, Manello JS, McGowan C, et al. Macromolecules 1985;18:1058.
[23] Schiang WR, Woo EP. J Polym Sci, Part A: Polym Chem 1993;31: 2081.
[24] Hayvali M, Gündüz H, Gündüz N, Kiliç Z, Hökelek T. J Mol Struc 2000; 525:215.
[25] Hunter CA, Sanders JKM. J Am Chem Soc 1990;112:5525.
[26] Yamamoto T, Fukushima N, Nakajima H, Maruyama T, Yamaguchi I. Macromolecules 2000;33:5988.
[27] Karangu NT, Rezac ME, Beckham HW. Chem Mater 1998;10:567.
[28] Chung IS, Kim SY. Macromolecules 2000;33:3190.
[29] Harris FW, Sakaguchi Y, Shibata M, Cheng SZD. High Perform Polym 1997;9:251.
[30] Rajesh CS, Capitosti GJ, Cramer SJ, Modarelli DA. J Phys Chem B 2001; 105:10175.
[31] Nappa M, Valentine JS. J Am Chem Soc 1978;100:5075.